Adipocyte Death, Adipose Tissue Remodeling, and Obesity Complications

Katherine J. Strissel, Zlatina Stancheva, Hideaki Miyoshi, James W. Perfield, II, Jason DeFuria, Zoe Jick, Andrew S. Greenberg, and Martin S. Obin

OBJECTIVE—We sought to determine the role of adipocyte death in obesity-induced adipose tissue (AT) inflammation and obesity complications.

RESEARCH DESIGN AND METHODS—Male C57BL/6 mice were fed a high-fat diet for 20 weeks to induce obesity. Every 4 weeks, insulin resistance was assessed by intraperitoneal insulin tolerance tests, and epididymal (eAT) and inguinal subcutaneous AT (iAT) and livers were harvested for histological, immunohistochemical, and gene expression analyses.

RESULTS—Frequency of adipocyte death in eAT increased from <0.1% at baseline to 16% at week 12, coincident with increases in *1*) depot weight; *2*) AT macrophages (ATMΦs) expressing F4/80 and CD11c; *3*) mRNA for tumor necrosis factor (TNF)-α, monocyte chemotactic protein (MCP)-1, and interleukin (IL)-10; and *4*) insulin resistance. ATMΦs in crown-like structures surrounding dead adipocytes expressed TNF-α and IL-6 proteins. Adipocyte number began to decline at week 12. At week 16, adipocyte death reached ~80%, coincident with maximal expression of CD11c and inflammatory genes, loss (40%) of eAT mass, widespread collagen deposition, and accelerated hepatic macrosteatosis. By week 20, adipocyte number was restored with small adipocytes, coincident with reduced adipocyte death (fourfold), CD11c and MCP-1 gene expression (twofold), and insulin resistance (35%). eAT weight did not increase at week 20 and was inversely correlated with liver weight after week 12 ($r = -0.85$, $P < 0.001$). In iAT, adipocyte death was first detected at week 12 and remained ≤3%.

CONCLUSIONS—These results implicate depot-selective adipocyte death and MΦ-mediated AT remodeling in inflammatory and metabolic complications of murine obesity. ***Diabetes*** **56: 2910–2918, 2007**

From the Obesity and Metabolism Laboratory, Jean Mayer-U.S. Department of Agriculture Human Nutrition Research Center on Aging (JM-USDA HNRCA) at Tufts University, Boston, Massachusetts.

Address correspondence and reprint requests to Martin S. Obin or Andrew S. Greenberg, USDA, HNRCA at Tufts University, Boston, MA 02111. E-mail: martin.obin@tufts.edu or andrew.greenberg@tufts.edu.

Received for publication 5 June 2007 and accepted in revised form 27 August 2007.

Published ahead of print at http://diabetes.diabetesjournals.org on 11 September 2007. DOI: 10.2337/db07-0767.

Additional information for this article can be found in an online appendix at http://dx.doi.org/10.2337/db07-0767.

AT, adipose tissue; ATMΦ, AT macrophage; AUC, area under the curve; CCR, C-C chemokine receptor; CLS, crown-like structure; DC, dendritic cell; DIO, diet-induced obesity; eAT, epididymal AT; HF, high fat; iAT, inguinal subcutaneous AT; IL, interleukin; ITT, intraperitoneal insulin tolerance test; LF, low fat; MCP, monocyte chemotactic protein; MGC, multinucleate giant cell; NEFA, nonesterified fatty acid; TNF, tumor necrosis factor.

Adipose tissue (AT) macrophages (ATMΦs) promote obesity-associated AT inflammation and insulin resistance (1–5). Infiltrating ATMΦs secrete proinflammatory mediators that are elevated in AT of obese mice and humans and are implicated in the development of insulin resistance, including tumor necrosis factor (TNF)-α, interleukin (IL)-6, and monocyte chemotactic protein (MCP)-1 (5–9). In obese mice and humans, MΦs infiltrate AT as circulating monocytes in response to AT secretion of MCP-1, which recruits monocytes expressing the C-C chemokine receptor (CCR)2 (1,2,10–12,13). CCR2+ MΦs expressing the MΦ differentiation marker F4/80 and CD11c, a dendritic cell (DC) marker (13) upregulated in MΦ foam cells (14), were recently reported to infiltrate AT of obese mice and were distinguished from noninflammatory resident ATMΦs (F4/80+/CCR2−/CD11c−) isolated from nonobese mice (12,15). However, the relationship between this obesity-associated ATMΦ "phenotypic switch" (12) and the development and progression of obesity complications is unclear (16,17).

In addition to their roles in innate immunity, MΦs perform vital functions in developmental and homeostatic tissue remodeling (18,19). In AT, MΦs promote angiogenesis and vascular remodeling required for postnatal growth of mouse epididymal AT (eAT) (20). ATMΦ production of matrix-degrading proteinases is implicated in the matrix remodeling associated with adipocyte enlargement and AT expansion (21). We previously hypothesized that infiltrating ATMΦs play an important role(s) in obesity-associated AT remodeling, based on our observation that ATMΦs in obese mice and humans localize to dead adipocytes, which increase in frequency in obesity (22). At sites of adipocyte death, ATMΦs aggregate to form a crown-like structure (CLS) that envelopes and ingests the moribund adipocyte and its potentially cytotoxic remnant lipid droplet (22). As a consequence of lipid scavenging, ATMΦs within CLS become lipid-laden "foam cells" (22). MΦ fusion within CLS is common, with multinucleate giant cells (MGCs) frequently observed (22). We propose that clearance of dead adipocytes by ATMΦs is an initial remodeling event required for AT repair and differentiation of new adipocytes at sites of adipocyte loss. MΦ-mediated cell killing is a feature of various forms of tissue remodeling (18), rendering it plausible that ATMΦs actively participate in adipocyte execution (22).

The clearance of dead adipocytes is likely to promote proinflammatory ATMΦ activation, reflecting both the necrotic-like morphology of adipocyte death and ATMΦ fusion (22). MΦ fusion, which synergistically increases MΦ absorptive capacity, requires TNF-α autocrine/paracrine signaling (23), suggesting that CLS and MGCs may be

TABLE 1
Primer sequences used for gene expression analysis by real-time PCR

Gene target	Sequences (5′–3′)
F4/80	F: CTTTGGCTATGGGCTTCCAGTC
	R: GCAAGGAGGACAGAGTTTATCGTG
CD11b	F: CGGAAAGTAGTGAGAGAACTGTTTC
	R: TTATAATCCAAGGGATCACCGAATTT
CD11c	F: CTGGATAGCCTTTCTTCTGCTG
	R: GCACACTGTGTCCGAACTC
CD68	F: CTTCCCACAGGCAGCACAG;
	R: AATGATGAGAGGCAGCAAGAGG
TNF-α	F: ATGGCGTTTCCGAATTCAC
	R: GAGGCAACCTGACCACTCTC
MCP-1	F: ACTGAAGCCAGCTCTCTCTTCCTC
	R: TTCCTTCTTGGGGTCAGCACAGAC
IL-6	F: TCCAGTTGCCTTCTTGGGAC
	R: GTGTAATTAAGCGCCGACTTG
Adiponectin	F: GAATCATTATGACGGCAGCA
	R: TCATGTACACCGTGATGTGGTA
Cyclophilin B	F: ATGTGGTTTTCGGCAAAGTT
	R: TGACATCCTTCAGTGGCTTG

F, forward; R, reverse.

chronic sources of TNF-α. Moreover, because each dead adipocyte "recruits" dozens of ATMΦs, a low frequency of adipocyte death may be sufficient to cause AT inflammation and promote insulin resistance. However, the proinflammatory milieu at sites of tissue remodeling is typically transient, giving way to a "repair" program that promotes resolution of inflammation and tissue restoration (24). Tissue repair is characterized by MΦ upregulation of anti-inflammatory mediators such as IL-10, IL-4, and TGF-β (24). Thus, the character, magnitude, and physiological impact of obesity-associated AT inflammation will in part reflect the net balance of proinflammatory and anti-inflammatory inputs during AT remodeling at sites of adipocyte death.

Here, using a 20-week course of high-fat (HF) feeding in C57BL/6 mice, we demonstrate that adipocyte death is an early, progressive, and depot-dependent event in diet-induced obesity (DIO) that is significantly correlated with AT expansion, the ATMΦ phenotypic switch, AT inflammation, and development of whole-body insulin resistance. Adipocyte death is prevalent in eAT, but not in inguinal AT (iAT), and is associated with matrix deposition and differentiation of new adipocytes. These observations suggest that obesity-associated remodeling in intra-abdominal AT contributes to inflammatory and metabolic complications of obesity (25,26).

RESEARCH DESIGN AND METHODS

Animals and diets. Experiments were conducted in a viral pathogen–free facility at the Jean Mayer-U.S. Department of Agriculture Human Nutrition Research Center on Aging at Tufts University in accordance with institutional animal care and use committee guidelines. At 5 weeks of age, individually caged male C57BL/6 mice (The Jackson Laboratories) were established in weight-matched groups fed either a low-fat (LF) diet (10% calories from fat; Research Diets no. D12450B) or a HF diet (60% calories from fat; Research Diets no. D12492) for 1, 4, 8, 12, 16, or 20 weeks.

Histology and immunohistochemistry. Mice were killed by CO_2 narcosis/cervical dislocation. Fat and liver were dissected, fixed, embedded in paraffin, and sectioned (22). Sections were stained with hematoxylin and eosin or with Gomori trichrome. Digital images were acquired with an Olympus DX51 light microscope. For each mouse, morphometric data were obtained from ≥500 adipocytes from three or more sections cut at least 50 μm apart. Immunohistochemistry was performed using VectaStain kits (Vector Labs). Antibodies were rat anti-mouse F4/80 (Serotec), Mac-2 (Cedarlane Labs), goat anti-mouse TNF-α, goat anti-mouse IL-6 (Santa Cruz), and rabbit anti-mouse perilipin (27). Negative controls were nonimmune IgG and peptide-neutralized primary antibody.

Adipocyte death. Dead/dying adipocytes were identified by light microscopy as perilipin-negative lipid droplets surrounded by MΦ crowns (22). The frequency of adipocyte death was calculated from micrographs as (number dead adipocytes/number total adipocytes) × 100.

Adipocyte volume and adipocyte number. Adipocyte volume was calculated from cross-sectional area obtained from perimeter tracings using Image J software (28) (Sun Microsystems). Adipocyte number was calculated from fat pad weight and adipocyte volume (29) and corrected for percentage of dead adipocytes.

Quantitative PCR. Adipose tissues (lymph nodes removed) were dissected, frozen in liquid nitrogen, and stored at −70°C. Total RNA was extracted, quantified, and analyzed by SYBR Green real-time PCR on an Applied Biosystems 7300 Real Time PCR system (30). Fold difference in gene expression was calculated as $2^{-\Delta\Delta Ct}$ using cyclophilin B as the endogenous control gene with mice fed the LF diet for 1 week as the "comparer" (31). Genes and primer sequences are listed in Table 1.

Measures of insulin resistance. Fasted (overnight) serum insulin was measured by enzyme-linked immunosorbent assay using mouse insulin as a standard (Crystal Chem). Intraperitoneal insulin tolerance tests (ITTs) were performed on nonanesthetized mice fasted for 4–6 h in the morning. Glucose measures were obtained from whole–tail vein blood using an automated glucometer at baseline and 15, 30, 45, 60, and 90 min following intraperitoneal injection of human insulin (0.75 mU/kg). Glucose area under the curve (AUC_{0-90}) was determined for HF-fed and LF-fed cohorts and the difference (ΔAUC) reported.

Biohumoral measures. Blood was obtained from fasted (overnight) mice by cardiac puncture. Serum leptin, resistin, adiponectin, and MCP-1 were measured by enzyme-linked immunosorbent assay (Lincoplex mouse adipokine; Millipore Bioscience), and nonesterified fatty acids (NEFAs) were measured using the NEFA-C kit (Wako Chemicals).

Statistics. ANOVA or general linear model procedures were used in conjunction with Tukey's honestly significant difference test (SYSTAT v10). Frequency data were transformed as $arcsin\sqrt{x}$ before statistical analysis. Significance was set at $P < 0.05$.

RESULTS

Adipocyte death is a continuous depot-dependent event during DIO-associated AT remodeling. DIO was established in male C57BL/6 mice during a 20-week course of HF feeding (Fig. 1*A*). Dead adipocytes were identified by combined F4/80 and perilipin immunohistochemistry (22) (Fig. 1*B*). The frequency of adipocyte death during the development of DIO was determined in histological sections of eAT and iAT obtained at weeks 1, 4, 8, 12, 16, and 20 (Fig. 1*C*). The frequency of adipocyte death in eAT increased progressively from <0.1% at week 1 to ~16% at week 12 (Fig. 1*C* and *D*). During this time, adipocyte death was robustly associated with adipocyte size ($r = 0.94$, $P < 0.001$), which increased (approximately sevenfold) through week 12 ($P < 0.001$) (Fig. 2*B*). Despite a relatively high rate of adipocyte death at week 12, no areas free of adipocytes were observed (Fig. 1*C*), and eAT mass continued to increase in the majority of mice examined (Fig. 2*D*). These observations demonstrate that the frequency of adipocyte death increases progressively during DIO and suggest that sites of adipocyte death are successfully remodeled to maintain AT integrity and expansion.

By week 16, however, the rate of adipocyte death in eAT was ~80% (Fig. 1*C* and *D*). At this time, many F4/80− stromal cells were observed in the interstitium between F4/80+ CLS (online appendix Fig. 1 [available at http://dx.doi.org/10.2337/db07-0767]). Gomori trichrome staining revealed collagen deposition proximal to both viable and dead adipocytes, consistent with active matrix remodeling at these sites (Fig. 1*E*). Both adipocyte number (Fig. 2*A*) and mean adipocyte size (Fig. 2*B*) decreased, and depot weight was reduced by 40% (Fig. 2*D*). Thus, at week 16, the

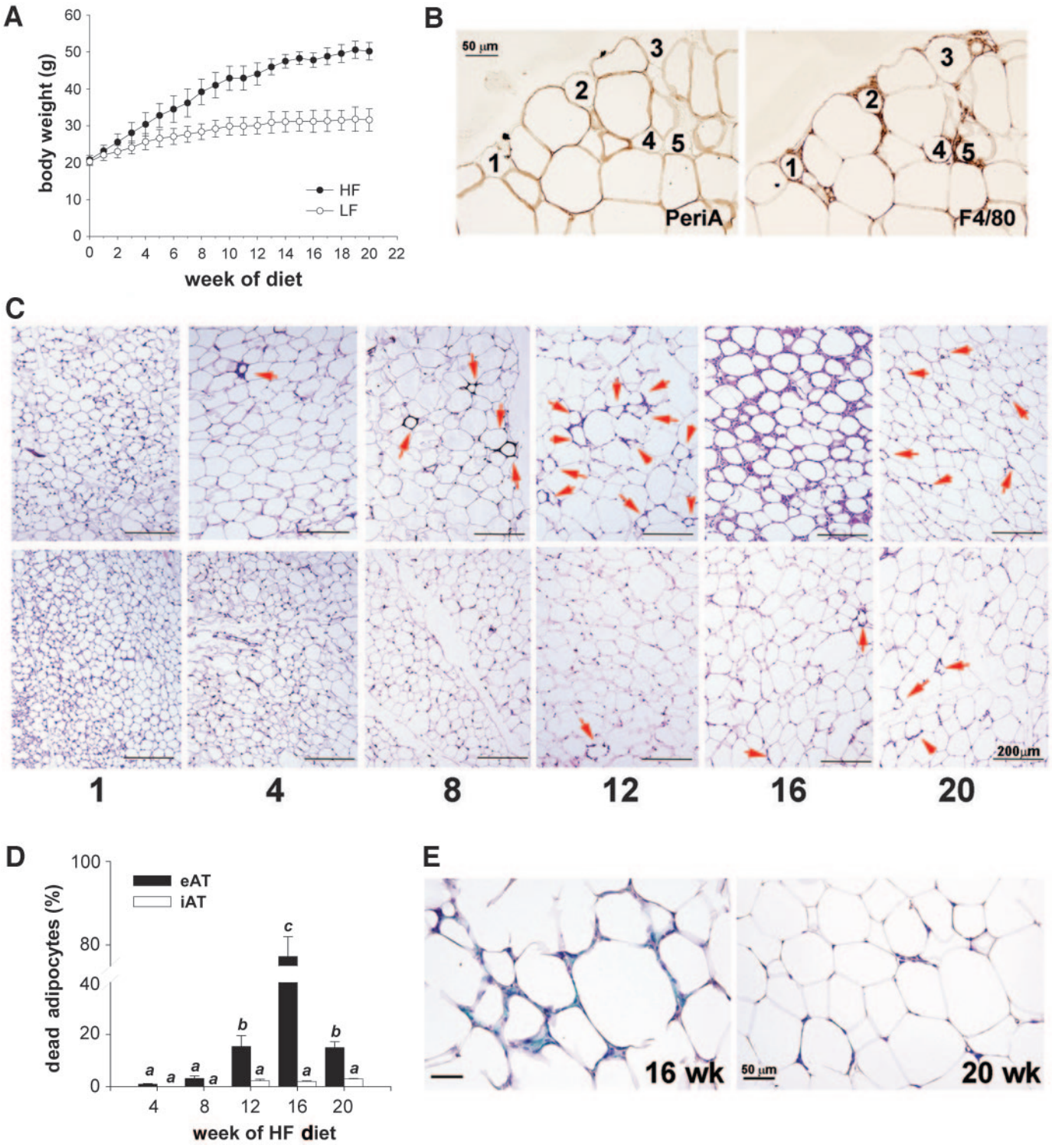

FIG. 1. Frequency and depot dependence of adipocyte death and AT remodeling during DIO. *A*: Mouse weight gain during 20 weeks of HF or LF feeding. *B*: Identification of dead adipocytes (numbered) as perilipin (PeriA)-negative lipid droplets surrounded by F4/80-positive cells (ATMΦs forming a CLS). *C*: Histology (hematoxylin and eosin–stained sections) of eAT and iAT showing CLS (arrows, except eAT at week 16 due to numerous CLS). *D*: Quantification of adipocyte death determined from multiple histological sections (>500 cells) of 6–8 mice/group/time point. Bars identified by the same letters are not significantly different ($P < 0.05$) by Tukey's procedure. *E*: Gomori trichrome staining reveals widespread collagen deposition (green) in the interstitium between adipocytes at week 16 but only infrequent collagen staining at week 20; dark blue/purple stain indicates nuclei; red/violet stain indicates cytoplasm, keratin, and muscle fibers.

rate of adipocyte death exceeded the rate of tissue repair resulting in net adipocyte and eAT loss.

By week 20, the frequency of adipocyte death had diminished fivefold to levels measured at week 12 (Fig. 1*D*), and adipocyte-free areas (Fig. 1*C*) and collagen staining of the interstitium between adipocytes (Fig. 1*E*) were rare. These observations indicate the resolution of remodeling with no apparent fibrosis. Notably, at week 20, adipocyte number of remodeled eAT was greater than fourfold the number observed at week 16 and was com-

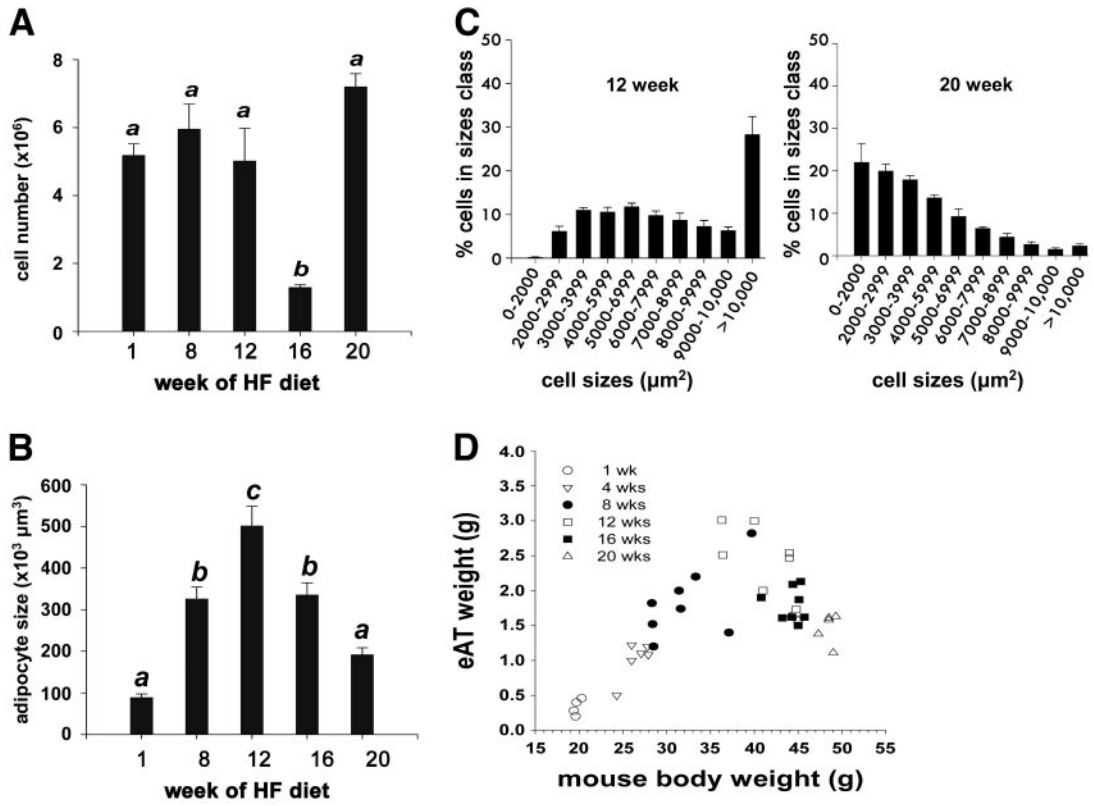

FIG. 2. Morphometric indexes of eAT remodeling during DIO. *A*: Adipocyte number. *B*: Adipocyte size (volume). Bars identified by the same letters are not significantly different ($P < 0.05$) by Tukey's procedure. *C*: Adipocyte size distribution showing the preponderance of small adipocytes in eAT at DIO week 20. Data for week 12 are included for comparison. *D*: eAT weight. Depot weight is expressed as a function of body weight. Data are from 4–6 mice (*A–C*) or 7–8 mice (*D*) at each time point.

parable to the adipocyte number at week 8 (Fig. 2*A*). A striking feature of remodeled eAT at week 20 was the prevalence of small adipocytes (Fig. 2*C*). As a consequence, eAT mass remained reduced as compared with week 12, despite restoration of adipocyte number (Fig. 2*A* and *D*). In control mice receiving the LF diet, the frequency of adipocyte death never exceeded 1% in eAT (data not shown).

In contrast to eAT, adipocyte death in iAT was not detectable until week 12 and never exceeded 3% ($P > 0.05$) (Fig. 1*C* and *D*). iAT mass increased continuously (>10-fold) throughout DIO, reflecting a 2-fold increase in adipocyte number ($P < 0.05$) and an ~3-fold increase in mean adipocyte size ($P < 0.05$) (online appendix Fig. 2*B*). The frequency of adipocyte death in iAT through week 20 was positively correlated with adipocyte size ($r = 0.86$, $P < 0.001$). However, maximal mean adipocyte size attained in iAT (211.6 ± 38.6 [$\times 10^3$ μm^3]) was less than half that measured in eAT (Fig. 2*B*). In control mice fed the LF diet, the frequency of adipocyte death in iAT did not exceed 0.5% (data not shown).

Serum levels of leptin and resistin (but not adiponectin) were elevated after one week of HF feeding and thereafter ($P < 0.001$ vs. LF-fed controls) (online appendix Fig. 3). Serum levels of adipokines were not significantly associated with the frequency of adipocyte death during the DIO time course. However, the twofold increase in serum leptin at week 20 ($P < 0.05$) was coincident with restoration of adipocyte number in eAT (Fig. 2*A*) and with continued expansion of iAT (online appendix Fig. 2*A* and *C*). Fasting serum NEFAs (online appendix Fig. 4) increased by week 8 ($P < 0.05$) and remained significantly elevated at week 12 in association with increased adipocyte size and AT mass (Fig. 2*B* and *D* and online appendix Fig. 2*B* and *C*); after week 12, fasting serum NEFAs eventually fell to levels measured at week 4, coincident with loss of eAT mass.

F4/80 and CD11c gene expression tracks the time course of adipocyte death in eAT. We next used real-time PCR analysis of AT to investigate associations between the onset and progression of adipocyte death and changes in ATMΦ marker gene expression. After 4 weeks of DIO, the ATMΦ phenotype was characterized by low expression of F4/80, CD11c, CD68, and CD11b (Fig. 3). These observations suggest that most ATMΦs present in eAT after 4 weeks of DIO are resident (CD11c−) ATMΦs. By DIO week 8, the expression of F4/80, CD11c, and CD11b began to rise (Fig. 3). These data are consistent with monocyte recruitment to eAT during the initial onset of adipocyte death (Fig. 1*D*) and with the subsequent differentiation of a subset of these monocytes into F4/80+/CD11c+ ATMΦs. F4/80, CD11c, CD11b, and CD68 gene expression (Fig. 3) tracked the increased frequency of adipocyte death between weeks 8 and 12 (Fig. 1*D*). As previously shown (22), foamy lipid-laden MΦs within CLS became frequent during this time (data not shown), potentially contributing to elevated CD11c expression by ATMΦs (14). Between weeks 12 and 20, the temporal pattern of ATMΦ marker gene expression became more dynamic and complex (Fig. 3). Whereas F4/80 expression remained elevated, CD11c expression diminished after week 16. CD11b expression fell progressively between weeks 12 and 20. In contrast, CD68 gene expression rose progressively through week 20 (Fig. 3) (see DISCUSSION).

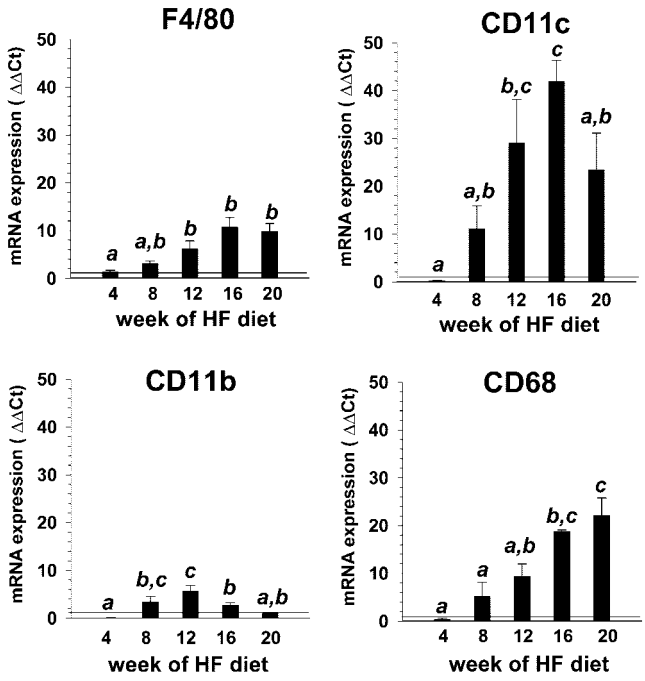

FIG. 3. Expression of MΦ marker genes in eAT during DIO. Real-time PCR data are expressed as fold difference (ΔΔCt) in gene expression relative to baseline (31) (see RESEARCH DESIGN AND METHODS). Data are from 4–6 mice/time point. Bars identified by the same letters are not significantly different ($P < 0.05$) by Tukey's procedure. Horizontal line indicates baseline gene expression.

In iAT, ATMΦ marker gene expression remained low throughout the DIO time course. We noted a modest (approximate twofold) upward trend in F4/80, CD68, and CD11c expression in iAT between weeks 12 and 20 (online appendix Fig. 2*D*), coincident with the onset of adipocyte death beginning at week 12 (Fig. 1*D*). Overall, however, the low frequency of adipocyte death in iAT (Fig. 1*C* and *D*) was associated with low ATMΦ gene expression.

Adipocyte death induces ATMΦ expression of proinflammatory hallmarks of obesity. If adipocyte death is an underlying cause of AT inflammation, CLS surrounding dead adipocytes should express inflammatory mediators that are upregulated in ATMΦs of obese mice. Moreover, the expression levels of these mediators should be positively associated with the frequency of obesity-induced adipocyte death in eAT. Immunohistochemistry (Fig. 4*A*) demonstrates expression of both TNF-α and IL-6 protein by ATMΦs arranged in CLS around remnant lipid droplets of dead adipocytes. Note that all ATMΦs within each CLS stain positive for the target cytokine. MGCs also expressed proinflammatory cytokines (Fig. 4*B*). Thus, scavenging of dead adipocytes is associated with ATMΦ expression of cytokines implicated in the development of insulin resistance.

Moreover, real-time PCR analysis of eAT revealed significant correlations between the frequency of adipocyte death and the expression of inflammatory mediators throughout the DIO time course (Fig. 5). Inflammatory mediators included TNF-α ($r = 0.78$, $P < 0.001$), which increased up to 10-fold ($P < 0.001$), IL-6 ($r = 0.48$, $P = 0.02$), which increased >2-fold ($P < 0.05$), MCP-1 ($r = 0.79$, $P < 0.001$), which increased ~7-fold ($P < 0.001$), and IL-10 ($r = 0.86$, $P < 0.001$), which increased ~15-fold ($P < 0.001$) (Fig. 5). Note that gene expression of each of these mediators was maximal at week 16 (coincident with maximal frequency of adipocyte death [Fig. 1*D*]) and then fell at week 20 to levels comparable with or approaching gene expression measured at week 12 (when the frequency of adipocyte death was comparable with that at week 20 [Fig. 1*D*]). Also note that IL-10 expression tracked the temporal pattern of TNF-α and MCP-1 expression (Fig. 5), indicating that anti-inflammatory mechanisms are upregulated in eAT, coincident with the progression of obesity-associated adipocyte death, ATMΦ recruitment, and proinflammatory gene expression.

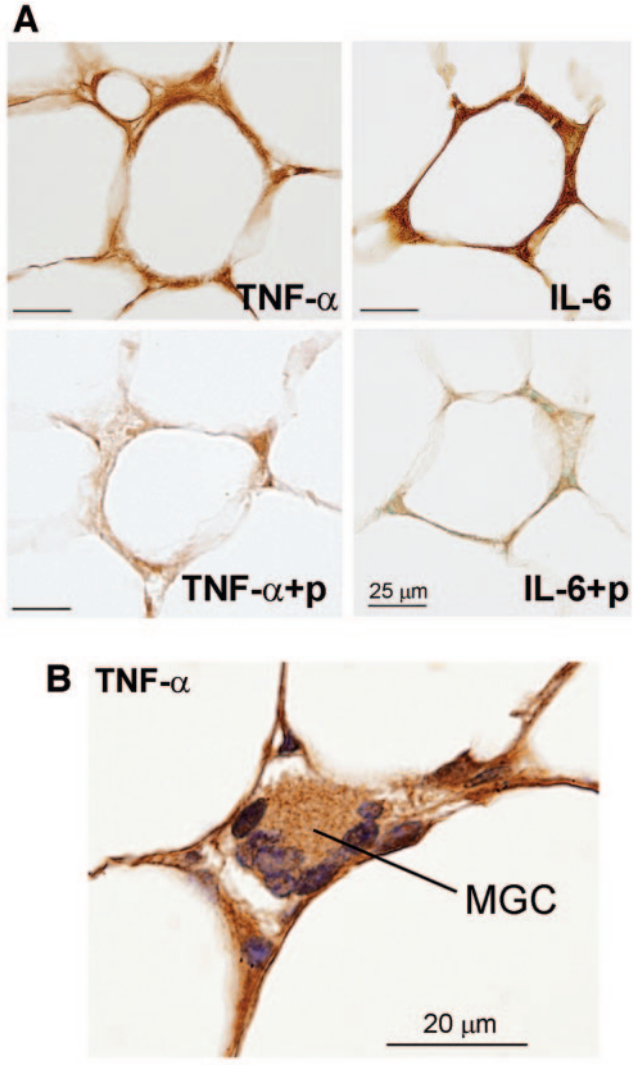

FIG. 4. Clearance of dead adipocytes by ATMΦs is proinflammatory. *A*: *Upper panels*: TNF-α and IL-6 immunohistochemistry reveals cytokine expression by CLS surrounding dead adipocytes in eAT of mice fed the HF diet for 8 weeks (above). *Lower panels*: Control sections preabsorbed with corresponding peptides (+p). *B*: TNF-α expression by a MGC associated with a CLS. Section was counterstained with hematoxylin.

In iAT, DIO-associated TNF-α gene expression was not detected until week 12 (data not shown), and its magnitude remained modest through week 20 (2.5 ± 0.2-fold, $P < 0.05$). Thus obesity-induced TNF-α gene induction was both delayed and attenuated in iAT as compared with eAT, consistent with the delayed time course and low frequency of adipocyte death (Fig. 1*C* and *D*). Similarly, IL-10 gene expression did not increase in iAT during the DIO time course and was comparable with levels measured in LF-fed mice (data not shown).

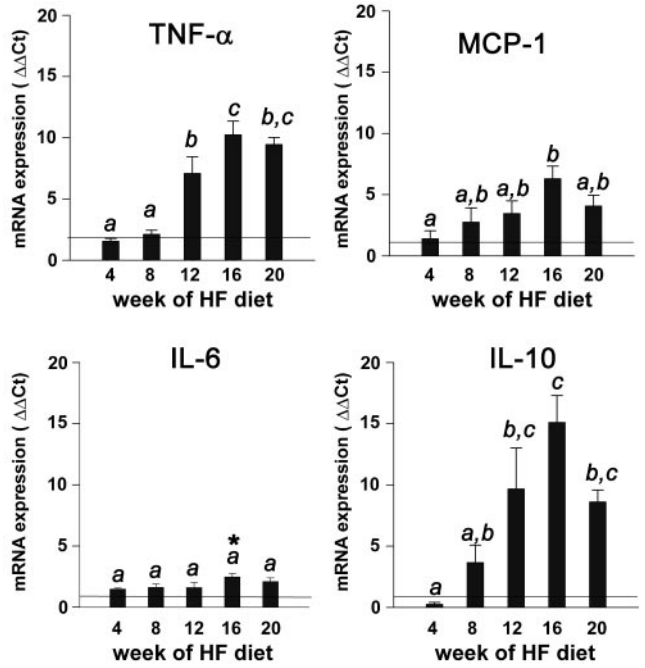

FIG. 5. Expression of inflammation-associated genes in eAT during DIO. Real-time PCR data are expressed as fold difference (ΔΔCt) in gene expression relative to baseline (31) (see RESEARCH DESIGN AND METHODS). Data are from 4–6 mice per time point. Bars identified by the same letters are not significantly different ($P < 0.05$) by Tukey's procedure. Horizontal line indicates baseline gene expression. Bar with asterisk indicates significantly different from baseline ($P < 0.05$).

Adipocyte death is associated with insulin resistance. The initial increase in adipocyte death in eAT between weeks 4 and 8 was coincident with the onset and progression of hyperinsulinemia and whole-body insulin resistance. At week 4, we detected nonsignificant trends for increased fasting serum insulin (Table 2) and for glucose AUC between HF-fed and LF-fed mice (ΔAUC) ($P > 0.05$) (Table 2). By DIO week 8, fasting insulin levels (Table 2) and homeostasis model assessment of insulin resistance values (not shown) were significantly elevated ($P < 0.01$), and whole-body insulin resistance was evident by ITT ($P < 0.001$) (Table 2). The development of whole-body insulin resistance by week 8 was coincident with upregulated expression of ATMΦ marker genes CD11b and CD11c (Fig. 3) and TNF-α (Fig. 5). Note that no increases in adipocyte death or ATMΦ infiltration were observed in iAT during the development of insulin resistance (Fig. 1*C* and *D*). Furthermore, insulin resistance was manifest at week 8 before the observed net loss of adipocytes detected in eAT beginning at week 12 (Fig. 2*B*). This observation argues against lipoatrophy as a contributing factor in the onset of systemic insulin resistance in this study. Fasting serum insulin levels remained essentially unchanged after week 8 (Table 2). However, insulin resistance continued to rise through week 12 ($P < 0.001$) (Table 2), coincident with attainment of maximal adipocyte size (Fig. 2*B*), increases in adipocyte death (Fig. 1*D*), increased expression of F4/80 (Fig. 3) and TNF-α (Fig. 5), and a threefold reduction in adiponectin gene expression (data not shown).

TABLE 2
Systemic insulin measures

Week of HF diet	ITT ΔAUC	Serum insulin (ng/ml)
1 week baseline	—	0.24 ± 0.08*
4	1,197.5 ± 583.3*	0.32 ± 0.09*
8	3,992.8 ± 486.9†	1.51 ± 0.19†
12	6,998.4 ± 900.6†‡	1.30 ± 0.0.39†
16	7,728.8 ± 663.9‡	1.12 ± 0.23†‡
20	4,628.7 ± 1143.0†	1.38 ± 0.18†

Data are means ± SE. Differences in ITT glucose AUC (ΔAUC) between HF-fed and LF-fed mice (n = 5–9) and fasted serum insulin in HF-fed mice (n = 4) during the DIO time course (see RESEARCH DESIGN AND METHODS). Means identified by the same symbol are not significantly different ($P < 0.05$) by Tukey's procedure.

Surprisingly, there was no significant increase in insulin resistance between weeks 12 and 16 (Table 2), although expression of ATMΦ marker genes in eAT remained elevated (Fig. 3), TNF-α gene expression increased (Fig. 5), and adiponectin gene expression was downregulated ~threefold (data not shown). However, fasting levels of serum NEFAs were significantly reduced at this time (online appendix Fig. 4). By week 20, insulin resistance was improved relative to week 16, with glucose ΔAUC obtained in the ITT of 20-week mice comparable with those obtained at week 8 (Table 2). This attenuated insulin resistance coincided with (partial) resolution of eAT remodeling, characterized by reduced frequency of adipocyte death (Fig. 1*D*), attenuated expression of CD11b and CD11c (Fig. 3), reduced adipocyte size and depot mass (Fig. 2*A*, *C*, and *D*), and further reductions in serum NEFAs (online appendix Fig. 4). However, F4/80 and TNF-α gene expression in eAT remained elevated at week 20 (Figs. 3 and 5), and adiponectin gene expression remained reduced relative to lean controls (data not shown).

eAT remodeling and hepatic steatosis. Clinical loss of adipose mass (lipoatrophy) is associated with hepatomegaly due to steatosis (32,33), as is chronic obesity. Beginning at week 12, DIO resulted in a progressive and significant loss of eAT mass (Fig. 2*C*). Moreover, this loss of mass was coincident with an accelerated increase in liver weight (Fig. 6*A*). Liver weight was robustly inversely associated with eAT weight beginning at week 12 ($r = -0.85$, $P < 0.001$) (Fig. 6*B*). Consistent with these observations, macrosteatosis was rare in livers of HF-fed mice up to week 12 but was widespread thereafter (Fig. 6*C*). These results suggest that loss of eAT mass due to remodeling may contribute to hepatic steatosis induced by HF-feeding.

DISCUSSION

The present study demonstrates that adipocyte death in eAT is an early and progressive event during DIO that is temporally linked to ATMΦ recruitment, the obesity-associated ATMΦ phenotypic switch (12), AT inflammation, and whole-body insulin resistance. The robust positive correlation between adipocyte size (Fig. 2*B*) and adipocyte death (Fig. 1*D*) during the initial 12 weeks of DIO suggests that adipocyte death may underlie the association of adipocyte size and ATMΦ infiltration in this and other studies (e.g., ref. 2). Notably, our results suggest that adipocyte death and clearance by ATMΦs are features of a homeostatic remodeling program that (at least initially) promotes AT expansion in response to energy surfeit. Additional components of this program include matrix remodeling (Fig. 1*E*) and vasculogenesis (20,21,34,35). ATMΦs are likely to be important mediators of these AT remodeling functions as well (18,19,21). Our data further

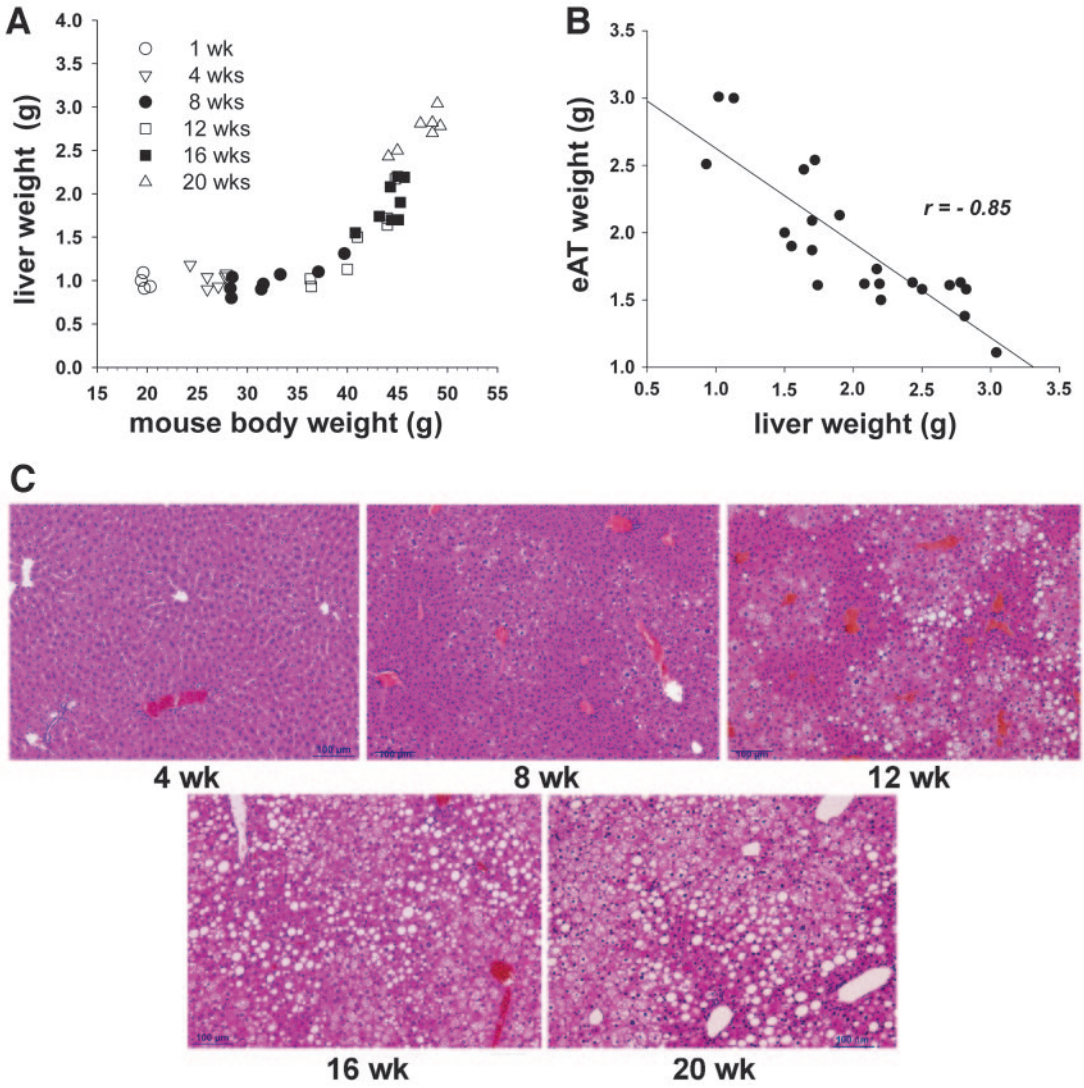

FIG. 6. Hepatic steatosis during DIO is associated with loss of eAT mass. *A*: Liver weight (adjusted for body weight) of mice fed a HF diet for 1, 4, 8, 12, 16, and 20 weeks. *B*: Inverse association of eAT mass and liver weight (as in *A*) between DIO weeks 12 and 20. *C*: Representative micrographs of hematoxylin and eosin–stained liver sections demonstrating that hepatic macrosteatosis in HF-fed mice is initially evident at DIO week 12 and increases through week 20.

suggest that later stages of eAT remodeling, characterized by net adipocyte and AT loss (subsequent to week 12 in the present study), are associated with phenotypic changes in ATMΦ subsets (reduced CD11b, increased CD68, and fluctuations in CD11c) and/or changes in numbers of non-MΦ cells expressing CD11b (e.g., monocytes), CD11c (e.g., DCs), and CD68 (e.g., stromal cells) (35,36).

A critical observation is that ATMΦs in CLS and associated MGCs express TNF-α and IL-6 protein (Fig. 4). This observation identifies dead adipocytes as important (although not necessarily exclusive) foci at which ATMΦs express proinflammatory hallmarks of obesity and insulin resistance. The relative persistence of F4/80 and TNF-α gene expression in eAT at week 20 (Figs. 3 and 5) suggests that ATMΦs promote obesity-associated inflammation in contexts in addition to adipocyte scavenging. However, the importance of adipocyte death in the development of obesity-associated AT inflammation and systemic insulin resistance is further supported by the observation that TNF-α, IL-6, and MCP-1 gene expression and the development of whole-body insulin resistance (assessed by ITT) were all significantly associated with the frequency of adipocyte death in eAT. These results implicate a role for adipocyte death and AT remodeling in the pathogenesis of obesity complications. At the same time, the relatively poor correlation between adipocyte death and serum adipokines (online appendix Fig. 3) indicates that the contribution of AT remodeling to obesity-associated pathology is but one piece of a complex puzzle involving many genes and metabolic pathways in multiple tissues.

IL-10 is an immunosuppressive cytokine secreted by MΦs and lymphocytes that promotes the resolution of inflammation and tissue repair, in part by blocking the proinflammatory actions of TNF-α (12,34). IL-10 gene expression was significantly upregulated in eAT during DIO (Fig. 5), tracking the frequency of adipocyte death as well as the magnitude of TNF-α and MCP-1 gene expression. This result is consistent with the demonstrated production of IL-10 by infiltrated CD11c+ ATMΦs isolated from obese (HF-fed) mice (12). However, IL-10 expression is reportedly greater in alternatively activated resident ATMΦs isolated from lean (LF-fed) mice (12). Thus, obesity-associated IL-10 gene expression in the present study may in part reflect increased numbers and/or upregulated

IL-10 expression by alternatively activated ATMΦs as well. Moreover, cells other than ATMΦs have the potential to contribute to and modulate the AT inflammatory profile during obesity-associated AT remodeling, including CD68+ stromal cells (36), DCs, lymphocytes (37,38), mesothelial cells (39), and adipocytes. These observations underscore the concept that obesity-associated eAT remodeling is a tightly regulated process involving coincident pro- and anti-inflammatory inputs from diverse and dynamic immune cell populations. The balance of these inputs ultimately accounts for the successful restoration of adipocyte number in eAT in the absence of fibrosis or adipocyte-free areas (Fig. 1*C* and *E*). Moreover, intervention strategies that shift the balance of these immune cell inputs toward a more anti-inflammatory (alternatively activated) set point may be effective in preventing or ameliorating inflammatory complications of obesity (12,40).

Our data additionally reveal depot selectivity in the frequency of obesity-associated adipocyte death, with eAT highly susceptible and iAT relatively resistant (Fig. 1*C* and *D*). These differences potentially reflect the relatively greater magnitude of adipocyte hypertrophy in eAT. Other intra-abdominal AT depots were also more susceptible to adipocyte death and infiltration of CD11c+ cells than iAT (online appendix Fig. 5). In general, intra-abdominal AT of rodents and humans is more susceptible to MΦ infiltration, is a greater source of inflammatory mediators, and may contribute more to some metabolic complications of obesity than subcutaneous AT (25,26,41–44). Removal of intra-abdominal AT in rodents ameliorates DIO-associated insulin resistance (26) and prevents insulin resistance and glucose intolerance of aging (25). Our results suggest that the pathogenicity of eAT and perhaps intra-abdominal AT in general may reflect susceptibility to obesity-associated adipocyte death. Although adipocyte hypertrophy is a correlate of this susceptibility (Fig. 2*B*), the proximate mediator(s) of obesity-associated adipocyte death is undetermined.

The reestablishment of adipocyte number at DIO week 20 with small adipocytes (Fig. 2*C*) suggested that adipocyte death may be a prerequisite for the transition from hypertrophic to hyperplastic obesity in eAT (45). However, we detected no increase in expression of the preadipocyte marker gene Pref-1 (46) at weeks 16 and 20 (data not shown). This suggests that the reestablishment of adipocyte number in eAT at week 20 may reflect nonclassical adipogenesis involving a preexisting pool of competent preadipocytes or other alternative mechanisms leading to new differentiated adipocytes (47,48). Reduced adipocyte size and loss of eAT mass at week 20 are also consistent with the proposal (49) that inflammatory ATMΦs function to limit fat expansion. In either case, reduced eAT mass subsequent to week 12 was associated with reduced fasting serum NEFAs (online appendix Fig. 4) and improved whole-body insulin resistance (Table 2), despite persistently elevated TNF-α gene expression (Fig. 5*A*). These salutary effects associated with reduced eAT mass potentially mimic the effects of eAT removal (see above). However, under conditions of chronic HF feeding, eAT reduction could contribute to lipid overflow to the liver (Fig. 6), potentially exacerbating hepatic insulin resistance (50) or promoting steatohepatitis.

In conclusion, adipocyte death and associated MΦ-mediated AT remodeling appear to be hallmark features of murine obesity that contribute to AT inflammation and whole-body insulin resistance. ATMΦ infiltration and activation are current targets of pharmacological interventions for obesity complications in humans. Determining whether and how these interventions modify AT remodeling remains a challenge for future studies.

ACKNOWLEDGMENTS

This work was supported by grants 5R01DK-50647 (to A.S.G.) and P30 DK046200-14 (to K.J.S.) from the U.S. Public Health Service, grant 1-06-RA-96 (to M.S.O.) from the American Diabetes Association, and by U.S. Department of Agriculture-Agricultural Research Service contract number 58-1950-7-707.

We thank Senait Assefa for expert assistance with animal husbandry, Annette Sheppard-Barry for histology services, and Drs. Rod Bronson and Robert Salomon for consultations. We also thank our colleagues and anonymous reviewers for their valuable comments on the manuscript.

REFERENCES

1. Xu H, Barnes GT, Yang Q, Tan G, Yang D, Chou CJ, Sole J, Nichols A, Ross JS, Tartaglia LA, Chen H: Chronic inflammation in fat plays a crucial role in the development of obesity-related insulin resistance. *J Clin Invest* 112:1821–1830, 2003
2. Weisberg SP, McCann D, Desai M, Rosenbaum M, Leibel RL, Ferrante AW Jr: Obesity is associated with macrophage accumulation in adipose tissue. *J Clin Invest* 112:1796–1808, 2003
3. Arkan MC, Hevener AL, Greten FR, Maeda S, Li ZW, Long JM, Wynshaw-Boris A, Poli G, Olefsky J, Karin M: IKK-beta links inflammation to obesity-induced insulin resistance. *Nat Med* 11:191–198, 2005
4. Lesniewski L, Hosch S, Neels J, de Luca C, Pashmforoush M, Lumeng C, Chiang S-H, Scadeng M, Saltiel A, Olefsky J: Bone marrow–specific Cap gene deletion protects against high-fat diet–induced insulin resistance. *Nat Med* 13:455–462, 2007
5. Cancello R, Clément K: Is obesity an inflammatory illness? Role of low-grade inflammation and macrophage infiltration in human white adipose tissue. *BJOG* 113:1141–1147, 2006
6. Kanda H, Tateya S, Tamori Y, Kotani K, Hiasa K-I, Kitazawa R, Kitazawa S, Miyachi H, Maeda S, Egashira K, Kasuga M: MCP-1 contributes to macrophage infiltration into adipose tissue, insulin resistance, and hepatic steatosis in obesity. *J Clin Invest* 116:1494–1505, 2006
7. Sell H, Kaiser U, Eckel J: Expression of chemokine receptors in insulin-resistant human skeletal muscle cells. *Horm Metab Res* 39:244–249, 2007
8. Senn JJ, Klover PJ, Nowak IA, Mooney RA: Interleukin-6 induces cellular insulin resistance in hepatocytes. *Diabetes* 51:3391–3399, 2002
9. Klover PJ, Clementi AH, Mooney RA: Interleukin-6 depletion selectively improves hepatic insulin action in obesity. *Endocrinology* 146:3417–3427, 2005
10. Takahashi K, Mizuarai S, Araki H, Mashiko S, Ishihara A, Kanatani A, Itadani H, Kotani H: Adiposity elevates plasma MCP-1 levels leading to the increased CD11b-positive monocytes in mice. *J Biol Chem* 278:46654–46660, 2003
11. Cancello R, Henegar C, Viguerie N, Taleb S, Poitou C, Rouault C, Coupaye M, Pelloux V, Hugol D, Bouillot JL, Bouloumie A, Barbatelli G, Cinti S, Svensson PA, Barsh GS, Zucker JD, Basdevant A, Langin D, Clement K: Reduction of macrophage infiltration and chemoattractant gene expression changes in white adipose tissue of morbidly obese subjects after surgery-induced weight loss. *Diabetes* 54:2277–2286, 2005
12. Lumeng CN, Bodzin JL, Saltiel AR: Obesity induces a phenotypic switch in adipose tissue macrophage polarization. *J Clin Invest* 117:175–184, 2007
13. Gordon S, Taylor P: Monocyte and macrophage heterogeneity. *Nat Rev Immunol* 5:953–964, 2005
14. Cho H, Shashkin P, Gleissner CA, Dunson DM, Jain N, Lee J, Miller Y, Ley K: Induction of dendritic cell-like phenotype in macrophages during foam cell formation. *Physiol Genomics* 29:149–160, 2007
15. Brake D, Smith E, Mersmann H, Smith C, Robker R: ICAM-1 expression in adipose tissue: effects of diet-induced obesity in mice. *Am J Physiol Cell Physiol* 291:C1232–C1239, 2006
16. Chen A, Mumick S, Zhang C, Lamb J, Dai H, Weingarth D, Mudgett J, Chen H, MacNeil DJ, Reitman ML, Qian S: Diet induction of monocyte chemoattractant protein-1 and its impact on obesity. *Obes Res* 13:1311–1320, 2005

17. Inouye KE, Shi H, Howard JK, Daly CH, Lord GM, Rollins BJ, Flier JS: Absence of CC chemokine ligand 2 does not limit obesity-associated infiltration of macrophages into adipose tissue. *Diabetes* 56:2242–2250, 2007
18. Lang R, Bishop J: Macrophages are required for cell death and tissue remodeling in the developing mouse eye. *Cell* 74:453–462, 1993
19. Duffield JS, Forbes SJ, Constandinou CM, Clay S, Partolina M, Vuthoori S, Wu S, Lang R, Iredale JP: Selective depletion of macrophages reveals distinct, opposing roles during liver injury and repair. *J Clin Invest* 115:56–65, 2005
20. Cho CH, Koh YJ, Han J, Sung HK, Jong Lee H, Morisada T, Schwendener RA, Brekken RA, Kang G, Oike Y, Choi TS, Suda T, Yoo OJ, Koh GY: Angiogenic role of LYVE-1-positive macrophages in adipose tissue. *Circ Res* 100:e47–e57, 2007
21. Huber J, Loffler M, Bilban M, Reimers M, Kadl A, Todoric J, Zeyda M, Geyeregger R, Schreiner M, Weichhart T, Leitinger N, Waldhausl W, Stulnig TM: Prevention of high-fat diet-induced adipose tissue remodeling in obese diabetic mice by n-3 polyunsaturated fatty acids. *Int J Obes* 31:1004–1013, 2006
22. Cinti SMG, Barbatelli G, Murano I, Ceresi E, Faloia E, Wang S, Fortier M, Greenberg AS, Obin MS: Adipocyte death defines macrophage localization and function in adipose tissue of obese mice and humans. *J Lipid Res* 46:2347–2355, 2005
23. Sorimachi K, Akimoto K, Tsuru K, Ieiri T, Niwa A: The involvement of tumor necrosis factor in the multinucleation of macrophages. *Cell Biol Int* 19:547–549, 1995
24. Duffield J: The inflammatory macrophage: a story of Jekyll and Hyde. *Clin Sci (Lond)* 104:27–28, 2003
25. Gabriely I, Ma XH, Yang XM, Atzmon G, Rajala MW, Berg AH, Scherer P, Rossetti L, Barzilai N: Removal of visceral fat prevents insulin resistance and glucose intolerance of aging: an adipokine-mediated process? *Diabetes* 51:2951–2958, 2002
26. Pitombo C, Araujo EP, De Souza CT, Pareja JC, Geloneze B, Velloso LA: Amelioration of diet-induced diabetes mellitus by removal of visceral fat. *J Endocrinol* 191:699–706, 2006
27. Souza SC, Yamamoto M, Franciosa M, Lien P, Greenberg A: BRL blocks the lipolytic actions of tumor necrosis factor-α (TNF-α): a potential new insulin-sensitizing mechanism for the thiazolidinediones. *Diabetes* 47:691–695, 1998
28. Rasband WS: Image J (software). Bethesda, MD, U.S. National Institutes of Health, 2006 (Available from http://rsb.info.nih.gov/ij)
29. Bourgeois F, Alexiu A, Lemonnier D: Dietary-induced obesity: effect of dietary fats on adipose tissue cellularity in mice. *Br J Nutr* 49:17–26, 1983
30. D'Eon TM, Souza SC, Aronovitz M, Obin MS, Fried SK, Greenberg AS: Estrogen regulation of adiposity and fuel partitioning: evidence of genomic and non-genomic regulation of lipogenic and oxidative pathways. *J Biol Chem* 280:35983–35991, 2005
31. Vandesompele J, De Preter K, Pattyn F, Poppe B, Van Roy N, De Paepe A, Speleman F: Accurate normalization of real-time quantitative RT-PCR data by geometric averaging of multiple internal control genes. *Genome Biol* 3:RESEARCH0034, 2002
32. Vigouroux C, Capeau J: A-type lamin-linked lipodystrophies. *Novartis Found Symp* 264:66–77, 2005
33. Grigem S, Fischer-Posovszky P, Debatin K, Loizon E, Vidal H, Wabitsch M: The effect of the HIV protease inhibitor ritonavir on proliferation, differentiation, lipogenesis, gene expression and apoptosis of human preadipocytes and adipocytes. *Horm Metab Res* 37:602–609, 2005
34. Zeyda M, Farmer D, Todoric J, Aszmann O, Speiser M, Gyori G, Zlabinger G, Stulnig T: Human adipose tissue macrophages are of an anti-inflammatory phenotype but capable of excessive pro-inflammatory mediator production. *Int J Obes (Lond)* 31:1420–1428, 2007
35. Nishimura S, Manabe I, Nagasaki M, Hosoya Y, Yamashita H, Fujita H, Ohsugi M, Tobe K, Kadowaki T, Nagai R, Sugiura S: Adipogenesis in obesity requires close interplay between differentiating adipocytes, stromal cells, and blood vessels. *Diabetes* 56:1517–1526, 2007
36. Khazen W, M'Bika J-P, Tomkiewicz C, Benelli C, Chany C, Achour A, Forest C: Expression of macrophage-selective markers in human and rodent adipocytes. *FEBS Lett* 579:5631–5634, 2005
37. Caspar-Bauguil S, Cousin B, Galinier A, Segafredo C, Nibbelink M, Andre M, Casteilla L, Penicaud L: Adipose tissues as an ancestral immune organ: site-specific change in obesity. *FEBS Lett* 579:3487–3492, 2005
38. Wu H, Ghosh S, Perrard XD, Feng L, Garcia GE, Perrard JL, Sweeney JF, Peterson LE, Chan L, Smith CW, Ballantyne CM: T-Cell accumulation and regulated on activation, normal T cell expressed and secreted upregulation in adipose tissue in obesity. *Circulation* 115:1029–1038, 2007
39. Darimont C, Avanti O, Blancher F, Wagniere S, Mansourian R, Zbinden I, Leone-Vautravers P, Fuerholz A, Giusti V, Mace K: Contribution of mesothelial cells in the expression of inflammatory-related factors in omental adipose tissue of obese subjects. *Int J Obes (Lond)* 2007 Jul 17 [Epub ahead of print]
40. Odegaard J, Ricardo-Gonzalez R, Goforth M, Morel C, Subramanian V, Mukundan L, Eagle A, Vats D, Brombacher F, Ferrante A, Chawla A: Macrophage-specific PPARgamma controls alternative activation and improves insulin resistance. *Nature* 447:1116–1120, 2007
41. Bashan N, Dorfman K, Tarnovscki T, Harman-Boehm I, Liberty IF, Bluher M, Ovadia S, Maymon-Zilberstein T, Potashnik R, Stumvoll M, Avinoach E, Rudich A: MAP kinases, IKK and insulin signaling in human omental versus subcutaneous adipose tissue in obesity. *Endocrinology* 148:2955–2962, 2007
42. Harman-Boehm I, Bluher M, Redel H, Sion-Vardy N, Ovadia S, Avinoach E, Shai I, Kloting N, Stumvoll M, Bashan N, Rudich A: Macrophage infiltration into omental versus subcutaneous fat across different populations: effect of regional adiposity and the co-morbidities of obesity. *J Clin Endocrinol Metab* 92:2240–2247, 2007
43. Yu R, Kim C-S, Kwon B-S, Kawada T: Mesenteric adipose tissue-derived monocyte chemoattractant protein-1 plays acrucial role in adipose tissue macrophage migration and activation in obese mice. *Obesity* 14:1353–1362, 2006
44. Cancello R, Tordjman J, Poitou C, Guilhem G, Bouillot JL, Hugol D, Coussieu C, Basdevant A, Hen AB, Bedossa P, Guerre-Millo M, Clement K: Increased infiltration of macrophages in omental adipose tissue is associated with marked hepatic lesions in morbid human obesity. *Diabetes* 55:1554–1561, 2006
45. Faust I, Johnson P, Stern J, Hirsch J: Diet-induced adipocyte number increase in adult rats: a new model of obesity. *Am J Physiol* 235:E279–E286, 1978
46. Kim K-A, Kim J-H, Wang Y, Sul HS: Pref-1 (preadipocyte factor 1) activates the MEK/extracellular signal-regulated kinase pathway to inhibit adipocyte differentiation. *Mol Cell Biol* 27:2294–2308, 2007
47. Crossno JT, Majka SM, Grazia T, Gill RG, Klemm DJ: Rosiglitazone promotes development of a novel adipocyte population from bone marrow-derived circulating progenitor cells. *J Clin Invest* 116:3220–3228, 2006
48. Nagayama M, Uchida T, Gohara K: Temporal and spatial variations of lipid droplets during adipocyte division and differentiation. *J Lipid Res* 48:9–18, 2007
49. Lacasa D, Taleb S, Keophiphath M, Miranville A, Clement K: Macrophage-secreted factors impair human adipogenesis: involvement of proinflammatory state in preadipocytes. *Endocrinology* 148:868–877, 2007
50. Choi CS, Savage DB, Kulkarni A, Yu XX, Liu Z-X, Morino K, Kim S, Distefano A, Samuel VT, Neschen S, Zhang D, Wang A, Zhang X-M, Khan M, Cline GW, Pandey SK, Geisler JG, Bhanot S, Monia BP, Shulman GI: Suppression of diacylglycerol acyltransferase-2 (DGAT2), but not DGAT1, with antisense oligonucleotides reverses diet-induced hepatic steatosis and insulin resistance. *J Biol Chem* 282:22678–22688, 2007